
AUTOMATIC IDENTIFICATION AND VISUALIZATION OF GROUP TRAINING ACTIVITIES USING WEARABLE DATA

Barak Gahtan¹, Shany Funk², Einat Kodesh², Itay Ketko³, Tsvi Kuffik², Alex M. Bronstein¹

¹Technion, Israel, ²University of Haifa, Israel, ³Israel Defense Forces (IDF)

{barakgahtan, bron}@cs.technion.ac.il,

{shanyfit, iketko}@gmail.com,

{ekodesh, tsviak}@univ.haifa.ac.il

ABSTRACT

Human Activity Recognition (HAR) is a crucial research area focused on identifying daily activities through the analysis of time-series data collected from wearable devices such as smartwatches. Recent advancements in Internet of Things (IoT), cloud computing, and low-cost sensors have broadened HAR applications across fields like healthcare, biometrics, sports, and personal fitness. However, challenges remain in efficiently processing the vast amounts of data generated by these devices and developing models that can accurately recognize a wide range of activities from continuous recordings, without relying on predefined activity training sessions. This paper presents a comprehensive framework for imputing, analyzing, and identifying activities from wearable data, specifically targeting group training scenarios without explicit activity sessions. Our approach is based on data collected from 135 soldiers wearing Garmin 55 smartwatches over six months. The framework integrates multiple data streams, handles missing data through cross-domain statistical methods, and identifies activities with high accuracy using machine learning (ML). Additionally, we utilized statistical analysis techniques to evaluate the performance of each individual within the group, providing valuable insights into their respective positions in the group in an easy-to-understand visualization. These visualizations facilitate easy understanding of performance metrics, enhancing group interactions and informing individualized training programs. We evaluate our framework through traditional train-test splits and out-of-sample scenarios, focusing on the model's generalization capabilities. Additionally, we address sleep data imputation without relying on ML, improving recovery analysis. Our findings demonstrate the potential of wearable data for accurately identifying group activities, paving the way for intelligent, data-driven training solutions.

1 Introduction

HAR is a research area focusing on identifying the daily activities carried out by individuals through the analysis of time series data collected from wearable devices such as smart watches. Significant advancements have been made over the last decade in the world of interconnected sensing technology, which includes sensors, IoT, cloud computing, and edge computing. Low-cost sensors can easily be incorporated or implanted into both portable and non-portable devices. As a result, a significant portion of HAR research has shifted its focus towards the use of these technologies. IoT-enabled wearable devices, equipped with sensors, can effectively capture and analyze various body movements, aiding in the identification and understanding of human activities [Lara and Labrador(2012)], [Ramanujam et al.(2021)], [Zhang et al.(2022)]. Affordable smartwatches equipped with wearable Inertial Measurement Units (IMU) sensors, which include accelerometers and gyroscopes, have resulted in the development of numerous applications across various domains, including healthcare [Kushwaha et al.(2021), Woznowski et al.(2016)], biometrics [Weiss et al.(2019)], sports analytics [Ramasamy Ramamurthy and Roy(2018)], personal fitness trackers [Ramasamy Ramamurthy and Roy(2018)]. The importance of HAR based on wearable devices becomes obvious since it can be used for classifying and logging many daily activities like walking, fast walking, running and detection of sleep. The challenge lies in effectively processing the vast amounts of data generated by these devices and developing robust models capable of accurately recognizing diverse activities under varying conditions, without explicit active

sessions. Another challenge that follows is how to effectively present the results of such models to end users in an intuitive and easy to understand way.

This paper presents an end-to-end framework for imputing, analyzing, and identifying every-day data collected from wearable devices, without the need for actively open training sessions. The framework allows for the identification of activities of soldiers and the visualization of an individual soldier relative to his team members that undergoes joint training over a specific duration, thereby making it understandable and accessible to end users through a simple yet informative display. The visualization effectively highlights whether an individual is overperforming or underperforming in comparison to the group.

To this end, 135 soldiers wore the same smart watch, Garmin 55, while performing the same schedule every day for approximately half a year. The proposed framework merges multiple data inputs onto a common grid, handles missing data points by leveraging information from different domains, rather than relying on traditional imputation methods. This enables us to fill in a large number of missing data in one domain using extended statistics from another domain, for example sleep imputation using heart rate (HR) inputs. Furthermore, it allows for accurate identification of various activities such as “Rifeling”, “Military drill”, “Fitness test”, “Running”, “Strength exercise”, “Krav maga” (Combative exercise), “Obstacle course training”, “Everyday activity” and “sleep”, without actively opening sessions on the smart watch. Therefore, the proposed framework provides a researcher with an automated preprocessing procedure for handling time-series data collected daily from the wearable device. Then, this data can be utilized for numerous downstream tasks, such as identifying the activity, identifying patterns among group training, and notifying when an individual is on track to get injured.

To evaluate the effectiveness of our framework, we conduct a series of experiments, including evaluations using both traditional train-test splits and more challenging out-of-sample scenarios. These experiments allow us to gauge the models’ generalization capabilities and their performance in recognizing activities on unseen days. Additionally, we address the imputation of missing sleep data, an essential component of accurately tracking and analyzing recovery periods without relying on ML techniques. Our findings demonstrate the potential of wearable data for accurately identifying activities, paving the way for more intelligent, data-driven training solutions. Finally, we offer an intuitive, easy to use visualization that enables end users to easily explore the results of the analysis, and see the relative position of an individual compared to his team member.

The rest of this paper is organized as follows: Section 2 reviews related work. Section 3 describes the automatic preprocessing and imputation stages, and then evaluates the ML models traditional way. Section 4 evaluates on out-of-sample days. Section 5 presents an automatic “smart” visualization for an individual relative standing within a group. Finally, Section 8 concludes the paper.

2 Related Work

HAR in group training settings utilizes advanced methods to identify activities conducted by groups rather than individuals, posing distinct difficulties in understanding collective actions. The utilization of hybrid techniques, such as the multilayer perceptron neural network in conjunction with IMU sensors, has exhibited remarkable precision in discerning specific activities by enhancing sensor data and employing Fast Fourier transform for feature extraction [Mao et al.(2023)]. Deep learning frameworks, specifically those that use graphical models, have been used in group settings to analyze the interactions between group members. These frameworks aim to capture both the actions of individuals and the overall behavior of the group [Salian and Kulkarni(2023)]. The active factor graph network model expands upon conventional second-order interactions to incorporate third-order interactions, thereby offering a more nuanced comprehension of group dynamics by taking into account the impact of pivotal individuals within the group [Xie et al.(2024)]. In addition, transfer learning models that utilize CNN architectures such as ResNet and MobileNet have achieved success in accurately identifying various activities by employing efficient feature extraction and majority voting fusion techniques [Jannat et al.(2023)]. Furthermore, the integration of multiple modes of wearable data provides an additional aspect to HAR.

Injury prediction using HR, steps, and sleep data entails combining biometric and activity metrics to predict potential injury risks. Predictive modeling is crucial in diverse fields such as sports and healthcare, as it enables timely intervention to avert serious consequences. A recent study employed ML methods to analyze heart rate variability (HRV) and found that spectral analysis of HRV can accurately forecast trauma outcomes. This indicates that these physiological measurements play a crucial role in evaluating the severity of injuries and predicting the course of recovery [Luo et al.(2021)]. In [Kleinsasser et al.(2022)] a study was conducted to examine the use of wearable devices such as Fitbits to predict sleep patterns. The study achieved a high level of accuracy in predicting sleep patterns and also demonstrated the potential for predicting other health-related events, such as injuries. In addition, ML models utilized on runners’ training logs, which include measurements such as steps taken and subjective effort, demonstrated a good

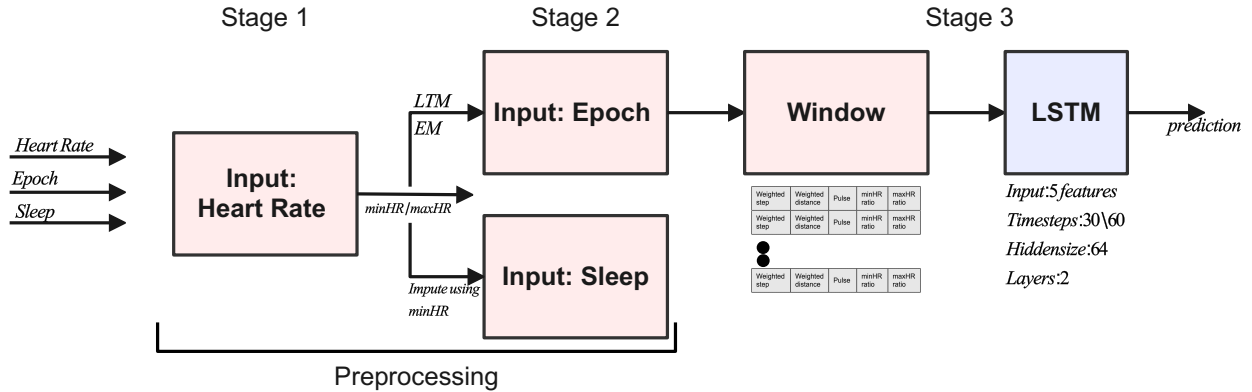


Figure 1: The data processing pipeline handles HR, epoch, and sleep inputs. It consists of three stages: preprocessing (Stage 1), windowing (Stage 2), and an identification LSTM model (Stage 3). The input data, including HR, epoch, and sleep records, are first fed into the preprocessing stage, then segmented into windows suitable for the LSTM model, which performs the prediction task.

ability to accurately predict injuries. This was especially evident when analyzing the training intensity leading up to the occurrence of injuries [Lövdal et al.(2021)]. Those findings of these studies suggest that the integration of HR, steps, and sleep data with advanced enough ML algorithms can establish reliable frameworks for predicting injuries.

Our work integrates wearable sensor data with ML to identify and analyze group training activities. We extend previous research by focusing on collective dynamics in military training, addressing missing data primary of sleep data, while utilizing multiple data streams.

3 Automatic Activity Imputation and Deep Learning Framework

Figure 1 shows the main stages of the proposed framework. In the first stage, HR data is used to compute personalized metrics that assist in managing the various sampling frequencies of the data. In Stage 2, these metrics are applied to project the different data modalities onto a common time grid. Stage 3 involves segmenting the features into windows suitable for input into the LSTM model, which is trained to predict outcomes. Each stage is described in detail below.

Data Collection and preprocessing Between September 4, 2022, and March 1, 2023, 135 soldiers wore the same smartwatch, Garmin 55, while living together and following a consistent daily schedule. Each participant signed an inform consent after an explanation about the study and volunteered to the study. The study was approved by Helsinki committee of the IDF’s Medical Corps ethical board (1998-2019) and by the Human Use Committee of Sheba Medical Center (6333-19-SMC). The collected dataset comprises all the raw data provided by Garmin, as specified in the Health REST API Specification [Garmin(nd)]. The primary data points we consider include heart rate (HR), epoch data (containing steps and distance covered), and sleep-related data. In the following section, we describe in detail the preprocessing steps applied to each of these subdomains, in order to combine them together using the same time grid.

Preprocessing heart rate measurements Garmin watches utilize photoplethysmography (PPG) sensors to monitor HR. These sensors operate by emitting light into the skin and detecting the amount of light absorbed or reflected back by the blood vessels. Variations in blood volume, caused by the heart’s pumping action, lead to fluctuations in light absorption, which the sensors capture to determine HR. This is a non-invasive technique. For HR data collection, Garmin wearables record measurements at intervals of every 15 seconds. We downsampled these measurements to a one-minute interval by averaging the pulse across every four samples.

Prior to downsampling, we calculated the minimum and maximum HR values for each day by identifying the 5th and 99.98th percentiles for each soldier. We then aggregated these daily values across the entire dataset to determine the median minimum and maximum HR for each individual referred to as *minHR* and *maxHR*. These metrics were then used to fill in gaps in the sleep data and accurately compute distances and steps taken during specific time intervals, as outlined below and shown in figure 1. This approach enables us to assess the relative effort exerted by each soldier based on their personalized HR metrics.

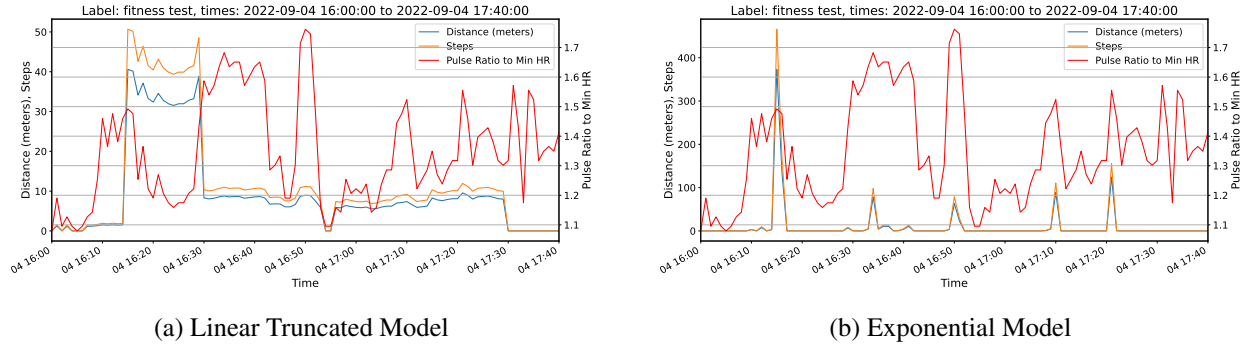


Figure 2: Time-series modeling comparing two different models during a fitness test. Figure (a) presents the output from the LTM, while Figure (b) shows the results from the EM. Both graphs depict the distance covered in meters, steps, and the pulse ratio relative to the minimum HR throughout the fitness test, which originally was in 15-minute interval. The left y-axes represent the distance (meters) and steps, while the right y-axis indicates the pulse ratio to minimum HR, which serves as a measure of cardiovascular effort relative to the individual’s baseline.

Preprocessing epoch measurements Garmin watches record distance covered and steps taken using a combination of accelerometer data and GPS tracking. The accelerometer estimates steps by measuring wrist movements and detecting changes in acceleration along different axes. However, when the arm is motionless or performing tasks that do not produce distinct movements, such as pushing a cart, this method may occasionally miss steps. GPS tracking is not utilized unless a specific activity is activated. Consequently, the watch relies solely on integrated sensors, such as the accelerometer, to estimate metrics like steps and distance, using either a standard or user-defined step length instead of actual GPS data.

The wearables collect measurements every 15 minutes for epoch data collection. To understand a person’s behavior on a per-minute basis in terms of steps and distance covered, we introduce two strategies: the Linear Truncated Model (LTM) and the Exponential Model (EM). These models ensure that HR, steps, and distance covered are all aligned on the same grid.

Linear Truncated Model: The LTM provides a straightforward approach that linearly correlates HR with physical activity metrics such as distance and steps. In this model, we use the $minHR$ parameter calculated for each individual, considering only data points where the pulse rate exceeds this threshold, multiplied by a factor of 1.1. Each minute’s contribution within a 15-minute interval is directly proportional to the pulse rate, with higher pulse rates resulting in proportionally greater contributions.

Exponential Model: The EM, on the other hand, employs a non-linear approach by exponentially weighting each minute’s contributions based on the pulse rate. Like the LTM, the $minHR$ threshold is used to filter out low-activity periods. However, above this threshold, the model disproportionately emphasizes higher pulse rates using an exponential function. This method is particularly beneficial for highlighting high-intensity activities, as it reflects the increased effort associated with higher pulse rates. The exponential weighting can more accurately capture the rapid escalation in physical output as intensity increases, which may not be as apparent in a linear model.

Figure 2 compares the same soldier’s fitness test data processed by the LTM and the EM. The figure shows (a) the LTM versus (b) the EM. In each plot, the left axis represents distance and steps, while the right axis corresponds to the pulse ratio relative to the $minHR$. The LTM provides a steady view of overall activity, aligning with the left axis, while the EM highlights intensity spikes, particularly on the right axis, where the exponential weighting emphasizes bursts of exertion. This contrast shows how the EM brings out high-intensity activities, whereas the LTM offers a more balanced depiction of sustained physical activity. Therefore, for evaluating, we use only the LTM model and do not use EM.

Preprocessing sleep measurements Garmin watches utilize built-in sensors to monitor various aspects of sleep, offering a comprehensive overview of a user’s sleep quality and patterns. The data collected encompasses the duration and different stages of sleep, including light, deep, and REM sleep, as well as periods of wakefulness. These insights are derived from continuous tracking of movement and HR variability, allowing the device to accurately detect transitions between various sleep stages.

The collected data includes the duration and stages of sleep, such as light, deep, and REM sleep, as well as periods of wakefulness. These findings are derived from continuous monitoring of movement and HR variability, enabling the device to detect transitions between different sleep stages.

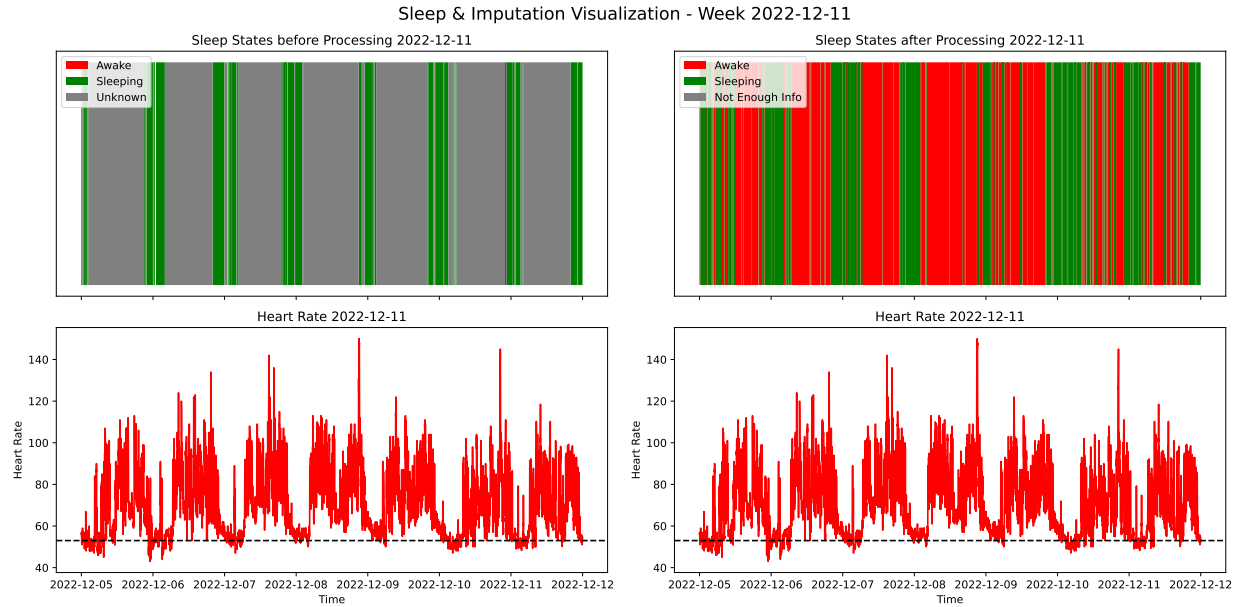


Figure 3: Visualization of sleep states and HR data before and after processing of a week time of a single soldier. The top part of the figure shows sleep states categorized as “Awake” “Sleeping” and “Unknown” before processing, and as “Awake” “Sleeping” and “Not Enough Info” after processing. The bottom part depicts HR data over the same time period, displaying fluctuations in heart rate across multiple days. The imputation process is reflected in the adjusted sleep states, providing a clearer distinction between sleep phases and periods of insufficient data.

To prepare the data for analysis, we first transformed the sleep stages, which are typically recorded within specific hour ranges, into one-minute intervals for each individual, assigning an associated category to each interval. For minutes without recorded data, we initially assigned a “?” to indicate missing data. Since Garmin watches do not track sleep during the day, we developed a method to intelligently impute missing data points both at night and during the day, allowing us to account for daytime sleep periods.

To impute missing data during the night, we utilized *minHR*. If a soldier’s pulse rate was below *minHR* and they had recorded zero steps during a given minute, that minute was labeled as sleep. For daytime hours, we adjusted the threshold, using a condition of $\text{pulse} \leq \text{minHR} \cdot 1.10$ to determine sleep. This allows us to impute missing data points, which we then verified against the planned schedule.

Additionally, we applied a second imputation technique using extrapolation. This involved identifying instances where five consecutive minutes had the same recorded value followed by a “?” and filling in the missing data with the value from the previous measurements. Finally, we categorized the data into three categories: “0” for awake, “1” for sleep, and “2” for unknown data points.

Figure 3 presents a side-by-side comparison of sleep state classification and HR data before and after imputation for the week starting on December 11, 2022. The visualization is divided into two sections. On the left, sleep states before processing display the original classification of sleep states, categorized as Awake (red), Sleeping, which includes light sleep, deep sleep, and REM, as recorded on the watch (green), and Unknown (grey), representing periods where the sleep state was not determined by the watch. On the right, sleep states after processing show the results after imputation, where unknown states have been reclassified as either Awake (red), Sleeping (green), or marked as Not Enough Info (grey), indicating periods where data is still insufficient even after processing. The x-axis represents time, spanning from December 5, 2022, to December 12, 2022, while the y-axis in lower plots represents HR. The HR data (red line) provides context on the individual’s physiological state during this period, while the horizontal dashed line is this specific soldier’s calculated *minHR* value. Notably, after imputation, gaps in sleep state classification are significantly reduced, with fewer unknown periods. This illustrates how the imputation process refines the data, filling in missing or uncertain sleep states, resulting in a more continuous and accurate representation of the individual’s sleep patterns.

Table 1 highlights the differences between the pre-processing and post-processing averages for the key metrics related to the completeness and quality of the sleep data. Before processing, the data contained a significant amount of

Metric	Pre-processing Averages	Post-processing Averages	Difference (Post - Pre)
Amount of data in minutes	78598.03	78598.03	0.00
Amount of filled sleep data	15034.03	41789.06	26755.03
Amount of filled awake data	610.66	35771.93	35161.27
Amount of missing data	62953.34	1037.05	-61916.29
Percent of data filled	18.44	95.11	76.67%
Percent of data missing	81.56	4.89	-

Table 1: Comparison of pre- and post-processing averages, including the difference between post- and pre-processing values.

missing information, with an average of 81.56% of the data being unfilled. We consider a data point as one minute. After applying our imputation techniques, the percentage of filled data increased dramatically from 18.44% to 95.11%, reflecting an improvement of 76.67%. Similarly, the amount of filled sleep data increased by 26,755.03 minutes (**about 18 days**), while the amount of filled awake data saw an even larger increase of 35,161.27 minutes (**about 24 days**). Conversely, the amount of missing data decreased significantly by 61,916.29 minutes. These results demonstrate the effectiveness of the imputation process in enhancing data completeness, thereby reducing the impact of missing data and allowing for more reliable insights into sleep behaviors. The appendix provides the data for each individual.

Dataset creation To apply supervised learning to time series data, it is essential to transform the data into input-output pairs. For this purpose, we employed the sliding window technique [Frank et al.(2001)], which requires specifying two parameters: the sliding window length and the sliding step. In our case, we used sliding window lengths of 30 and 60 minutes, resulting in training samples with 30 and 60 rows of multiple features, respectively. During training, we applied a 90% overlap between consecutive windows, corresponding to 27 and 54 minutes, to maximize the number of training samples. Since the data labels are derived from the soldiers’ schedules, the labels differ in both length and timing. For a label to be assigned to a specific window, it must be continuous for at least the duration of the window (either 30 or 60 minutes). This ensures that each window in the dataset is accurately labeled according to the corresponding schedule.

Evaluating the models To illustrate the practical capabilities of our models, we first show an evaluation using an 80:20 train-test split, where 80% of the data was utilized for training and the remaining 20% was reserved for testing on out-of-sample data. This initial evaluation allowed us to assess the model’s generalization capabilities. In the following section, we further extend the evaluation to include out-of-sample days, providing a more comprehensive analysis of the model’s performance. The dataset used for these evaluations is based solely on heart-rate and epoch-related data to identify various activities. For sleep identification, we provide statistics on the successful imputation of sleep times, achieved without the use of machine learning techniques.

The input data was preprocessed as described earlier and further segmented into sequences of features using a sliding window approach. To mitigate class imbalance within the dataset, we applied the Synthetic Minority Over-sampling Technique (SMOTE) [Chawla et al.(2002)], a widely recognized method for generating synthetic instances of minority classes. By augmenting the dataset with these additional examples, SMOTE effectively balanced the training data, thereby improving the model’s ability to accurately classify activities that were previously underrepresented.

The ML model’s architecture is based on a Long Short-Term Memory (LSTM) network [Yu et al.(2019)], which excels at processing sequential data. The input layer is designed to handle five key features: *pulse*, *steps per minute*, *distance covered per minute*, *pulse min ratio*, and *pulse max ratio*. The pulse min and max ratios were computed during preprocessing by dividing the pulse for each minute by the respective *minHR* or *maxHR* values. In the windowed dataset, timestamps are intentionally excluded, as the windows represent relative time intervals of 30 or 60 minutes, ensuring the model focuses on activity recognition without being tied to specific times. After the input layer, which extracts relevant features while preserving the temporal sequence, LSTM layers are utilized to capture the inherent temporal dependencies in the data. The model concludes with a fully connected output layer that translates these learned temporal patterns into activity classifications. The architecture includes two LSTM layers, each containing 64 neurons.

The model was trained with a batch size of 32, using the Adam optimizer [Kingma and Ba(2014)] and the ReduceLROnPlateau learning rate scheduler. This scheduler tracks the validation loss and reduces the learning rate by 50% when a plateau is detected, allowing for finer adjustments during training. To prevent overfitting, early stopping was applied, with a patience of ten epochs, meaning training was stopped if the validation loss did not improve over ten consecutive epochs. After training, the model was evaluated on a test set, which constituted 20% of the original dataset. The evaluation involved comparing the predicted labels with the true labels to assess model performance.



(a) 30-minute window length

(b) 60-minute window length

Figure 4: Confusion matrices comparing the performance of activity recognition models using two different sliding window lengths. (a) presents the results for the 30-minute window length, while (b) shows the results for the 60-minute window length. The matrices display the predicted activities on the x-axis and the true activities on the y-axis. The color shading reflects the proportion of correct and incorrect predictions, with darker shades representing higher values. The bar on the right shows the corresponding color scale for the prediction proportions.

Figure 4 presents two confusion matrices for two different sliding window lengths of 30 minutes and 60 minutes, respectively, for the same set of activities. The matrices show the models’ performance in predicting each activity, highlighting how the choice of window length impacts classification accuracy. Each matrix is normalized to show the percentage of predictions. The color intensity within each matrix reflects the proportion of correctly and incorrectly classified instances, allowing for a direct comparison between the two window lengths in terms of model accuracy across the activities.

Figure 4(a) shows that the model trained with a 60-minute sliding window length generally exhibits higher accuracy across most activities compared to the model trained with a 30-minute window. For example, the accuracy for “Everyday Activity” with the 60-minute model is 82.28%, significantly outperforming the 62.53% accuracy achieved by the 30-minute model. This trend is consistent across activities such as “Rifle Drill” where the 60-minute model achieves an accuracy of 70.18%, compared to 55.91% for the 30-minute model. The rest of the activities between the two window lengths are comparable. Lastly, the 60-minute model shows a marked improvement in reducing misclassification, as seen in the lower percentages of confusion between similar activities. These results indicate that while the 60-minute model is generally more accurate, the 30-minute model could still be preferable for specific, more detailed activity recognition tasks, that are generally known to be shorter. We can see that using a 30-minute window length, we have activities such as “Obstacle Training” that do not exist in the 60-minute window, since they do not take more than 60-minute, therefore those do not have a label when using a 60-minute sliding window.

4 Evaluation

In this section, we extend the evaluation of our models to more challenging scenarios by testing on out-of-sample days. Unlike traditional train-test splits that may include temporal overlap or shared characteristics between training and testing data, these evaluations are designed to assess the models’ robustness and generalization capabilities under conditions where the testing data is entirely unseen during training. By focusing on out-of-sample days, we examine the model’s ability to accurately recognize activities on days that were not part of the training process, reflecting real-world scenarios where data may vary over time. To this end, we sampled days that were not part of the training and fragmented those days into non-overlapping windows, either using 30-minute or 60-minute windows.

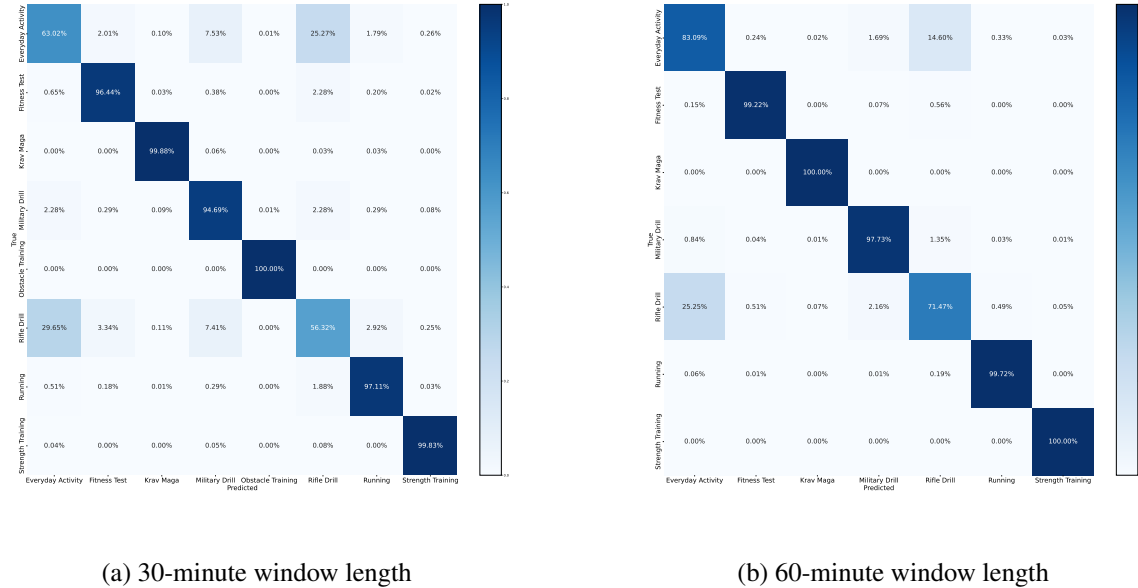


Figure 5: Confusion matrices comparing the performance of activity recognition models using two different sliding window lengths, on out of sample days.

Figure 5 presents a comparison between using 30-minute (Figure 5(a)) and 60-minute (Figure 5(b)) sliding windows. The 30-minute window offers a more detailed, fine-grained segmentation, which could enhance the model’s ability to distinguish between activities. However, this granularity comes with the trade-off of potentially fragmenting longer activities across multiple windows, leading to incomplete or less accurate classification results. In contrast, the 60-minute window captures broader data segments, which may be better suited for identifying longer activities, but it risks losing critical detail for shorter activities, affecting the overall classification performance. Again the figure shows that using a 30-minute window length, we have activities such as “Obstacle Training” that do not exist in the 60-minute window.

As the figure shows, the 60-minute window demonstrated a higher overall classification accuracy across most categories compared to the 30-minute window. In particular, the “Everyday Activity” and “Military Drill” categories showed a significant improvement in classification accuracy with the longer window. The longer 60-minute window provides better stability and recognition of everyday activities, potentially due to the extended temporal context that captures the variability of movements over time. The 30-minute window, on the other hand, appears to confuse Everyday Activity with Running, which shares some movement patterns.

For the “Everyday Activity” category, the 60-minute window achieved 83.09% accuracy, with most misclassifications occurring with “Rifle Drill” (14.60%) and “Military Drill” (1.69%) Figure 5(b). In contrast, the 30-minute window showed a marked decrease in accuracy to 63.02%, with major misclassifications into “Running” (25.27%) and “Military Drill” (7.53%) Figure 5(a). This suggests that a longer window helps in capturing the necessary temporal context to distinguish between activities with overlapping movement patterns. Similarly, for “Rifle Drill”, the 60-minute window showed an accuracy of 71.47%, while the 30-minute window struggled with 56.32%. This demonstrates that activities involving repetitive movements, like drills, benefit from a longer window to capture contextual cues.

The results of the out-of-sample day evaluations are notably similar to those observed in the traditional 80:20 train-test split. This consistency can be attributed to the nature of the data, where individuals are performing structured group activities. As a result, the patterns observed during each activity tend to remain consistent across different days, even though the specific time windows may vary. This suggests that the model is capable of generalizing well to unseen data, likely due to the repetitive nature of the activities being performed, which allows for the recognition of distinct movement patterns, irrespective of the exact day on which they occur.

5 “Smart” visualization for an individual relative standing in a group

In the context of analyzing physical performance data from individuals, it is essential to develop smart visualization tools that can reveal insights into how individuals perform relative to a group. This provides a clear, intuitive way to assess whether an individual is underperforming or overperforming in specific activities, highlighting areas of improvement or concern. Second, group-level comparisons can help track overall trends, ensuring that individual performance is assessed fairly relative to group norms rather than in isolation. Finally, visualizing relative performance can aid in setting individualized training plans, ensuring that each individual is progressing at their own optimal rate while benchmarking against the group.

The following figures illustrate the relative performance of randomly selected individuals compared to the group across three different activities: a *fitness test*, a *military drill*, and *rifling*. Each radar chart provides a visual comparison of five key metrics: *distance per minute*, *steps per minute*, *pulse per minute*, *pulse to min ratio*, and *pulse to max ratio*. The percentages in the radar graph represent normalized values of the performance metrics, ranging from 0% to 100%. These values are scaled relative to the maximum possible or observed values for each metric, allowing for comparison across different metrics with potentially different units (e.g., steps per minute, distance covered, HR). The values presented for the group performance reflect the median across all soldiers for that activity.

In each radar chart, the solid blue line represents the individual’s median performance across all metrics, while the solid red line indicates the group’s median values. The shaded areas surrounding the lines indicate the range or variance in the data: the blue shaded area corresponds to the variability in the individual’s performance, and the red shaded area reflects the group’s variability. The extent of the shaded area highlights the degree of variability across the metrics. Larger shaded areas indicate higher variability, while smaller areas suggest more consistent performance. This visualization enables easy identification of whether an individual is overperforming or underperforming relative to the group and provides insight into performance stability.

A higher pulse-to-max ratio indicates that the individual is exerting more effort, as their current pulse is closer to their maximum calculated pulse, implying greater cardiovascular strain. In contrast, a lower pulse-to-min ratio indicates better efficiency, as the current pulse is closer to the individual’s minimum calculated pulse. A higher pulse-to-min ratio suggests that the individual is farther from their resting HR, indicating they are working harder during the activity.

Across the three activities presented in Figure 6, the performance of different individuals varies significantly based on their physiological responses to the actions performed. In the fitness test (Figure 6(a)), the individual’s pulse-to-max ratio is slightly lower than the group’s, suggesting they exerted slightly less cardiovascular effort relative to their maximum. In terms of distance and steps, the individual covered the same as the group.

For the military drill (Figure 6(b)), however, the individual demonstrates a different performance pattern. The considered individual has a slightly higher pulse-to-max ratio than the group, meaning they worked harder in terms of cardiovascular effort, for the same activity volume.

In the rifling activity (Figure 6(c)), a different individual underperforms relative to the group, showing lower physical activity (in terms of steps and distance covered) and exerting less cardiovascular effort, as indicated by their lower pulse-to-max ratio. This lower engagement in the task requirements needs to be further investigated by the supervisors. These results emphasize how individual performance can vary across different activities, suggesting the potential for tailored interventions to boost both physical output and cardiovascular exertion during specific tasks.

Such visualizations are particularly valuable in online monitoring systems, where they can offer real-time feedback on individual performance relative to a group. In scenarios such as military training, the ability to visualize both physical and cardiovascular performance can help supervisors identify where individuals are excelling or underperforming. These radar charts, for example, provide a clear and an easy-way to compare an individual’s output with the group’s median values, making it easier to identify trends that might not be obvious from raw data alone.

Moreover, by visualizing performance across multiple metrics, these charts allow for the detection of inefficiencies or areas that require further development. For example, an individual who performs well physically but underutilizes their cardiovascular capacity, as seen in the military drill case, could be pushed to enhance their cardiovascular endurance. Similarly, individuals who consistently underperform in certain activities, like the rifling example, could be given targeted interventions to improve their engagement and output.

These visual tools support adaptive training in real-time. In highly dynamic environments where continuous monitoring is critical, such as military operations, online monitoring systems can use visualizations to adjust training intensity in real time. If an individual is found to be underexerting relative to the group, supervisors can increase the challenge, while overexertion can be flagged to reduce the risk of injury. Additionally, such monitoring enables personalized

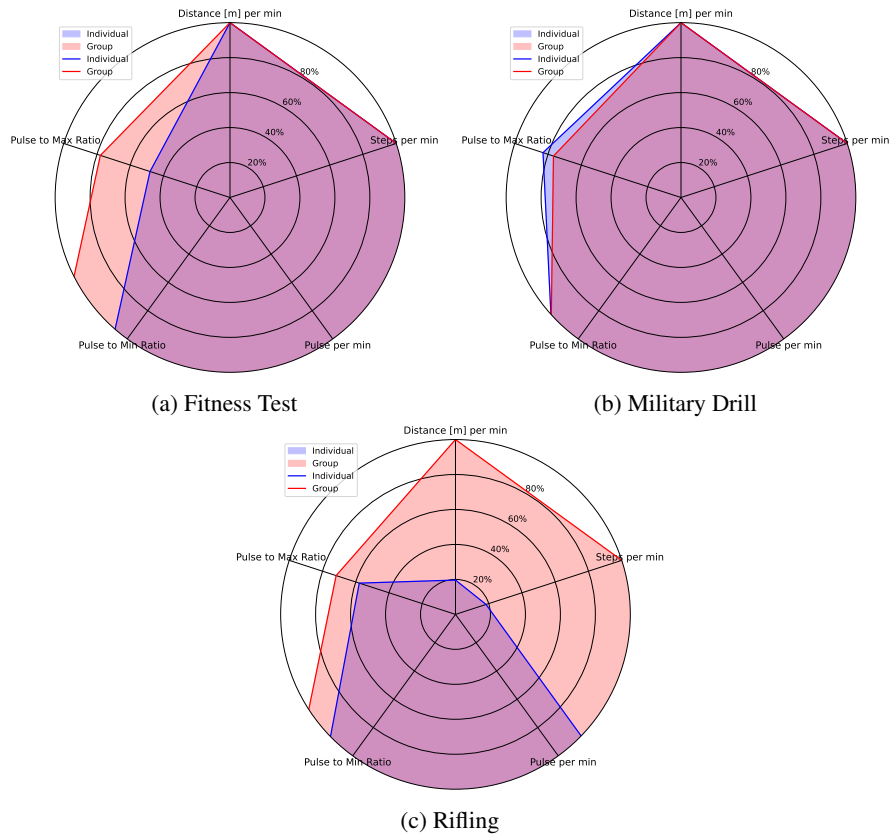


Figure 6: The performance of an individual computed across different tasks (a-c), represented by the blue line, relative to the group median (represented by the red line) across multiple metrics, including distance covered per minute, steps per minute, and pulse ratios. The solid lines represent the median values for the individual and the group across these metrics. The shaded areas surrounding each line represent the range or variance of the data for both the individual and the group. The larger the shaded area, the more variability exists in the data for that metric, providing insight into consistency across the metrics

training, where insights drawn from the visualization can guide the development of tailored training programs that address specific weaknesses or maximize strengths.

6 Discussion

The results presented highlight the efficacy of wearable data in identifying and classifying activities with high accuracy. By leveraging HR, steps, and sleep data from wearable devices, we were able to automate the identification of activities across multiple time windows. Our framework demonstrated significant improvements in the recognition of diverse activities, particularly in longer time windows, where the context from extended data improved the overall classification performance. One of the primary implications of our work is the potential for enhancing individualized training programs in group settings. The ability to track both individual and group performance in real-time opens up new possibilities for optimizing training regimes, preventing injury, and improving recovery. In addition, the integration of imputed sleep data allows for a more comprehensive analysis of recovery periods, which is critical for ensuring the physical readiness of soldiers or athletes undergoing intensive training.

However, we do need to acknowledge several limitations. First, while the imputation techniques for missing sleep data yielded accurate results, these methods did not utilize ML and required a statistical calculation of a soldier's minimum HR recorded over a high number of days. Thus, this may not generalize well in other contexts or with other data sources that exhibit different patterns. Additionally, the classification models may struggle with activities of shorter duration, where a 60-minute window could obscure the finer-grained details needed to differentiate between activities, consider brief running sessions that last only a few minutes. Lastly, the wearable devices used in this study have

inherent limitations, such as occasional step miscounts or unreliable data, as well as missing data points when soldiers did not wear their watches. These factors may have impacted the overall activity classification’s precision.

7 Acknowledgments

This study was supported by a grant from the Israel Defense Forces (IDF) Medical Corps and the Directorate of Defense Research and Development, Israeli Ministry of Defense (DDRD-MOD) (#4441028401). The funders had no role in study design, data collection and analysis, publication decisions, or manuscript preparation.

8 Conclusion and Future Work

We proposed a framework for automatic identification and visualization of training activities using wearable data, focusing on real data composed of HR, steps, and sleep. The results demonstrated that longer time windows offer better classification performance, especially for activities that involve repetitive movements or extended time frames. Our imputation techniques also enhanced the quality of the data, particularly in filling missing sleep states, allowing for more accurate tracking of recovery periods.

The framework not only automates activity identification but also facilitates easy-to-understand visualization in group training scenarios, contributing to the overall efficiency of training programs. By providing relative visualization of individuals within the group, it offers valuable insights that can be used to enhance the overall training strategy.

Future research can build upon these results by integrating advanced ML models for imputation or data generation to fill in missing data. For example, using a generative adversarial network [Goodfellow et al.(2020)] to fill in missing data points that were not collected. Furthermore, exploring the use of hybrid time windows, which dynamically adjust based on the type of activity, could provide a more flexible solution for activity recognition instead of using fixed window lengths. Lastly, expanding this framework to real-time use in training programs along with injury prediction models that use both HR and sleeping data could open up new ways for wearable data to be used in military and sports training.

References

- [Chawla et al.(2002)] Nitesh V Chawla, Kevin W Bowyer, Lawrence O Hall, and W Philip Kegelmeyer. 2002. SMOTE: synthetic minority over-sampling technique. *Journal of artificial intelligence research* 16 (2002), 321–357.
- [Frank et al.(2001)] Ray J Frank, Neil Davey, and Stephen P Hunt. 2001. Time series prediction and neural networks. *Journal of intelligent and robotic systems* 31 (2001), 91–103.
- [Garmin(nd)] Garmin. n.d.. Garmin Health API. <https://developer.garmin.com/gc-developer-program/health-api/> Accessed: 2024-08-01.
- [Goodfellow et al.(2020)] Ian Goodfellow, Jean Pouget-Abadie, Mehdi Mirza, Bing Xu, David Warde-Farley, Sherjil Ozair, Aaron Courville, and Yoshua Bengio. 2020. Generative adversarial networks. *Commun. ACM* 63, 11 (2020), 139–144.
- [Jannat et al.(2023)] Miskatul Jannat, Rezwana Karim, Navia Zafrin Islam, Abu Nowshed Chy, and Abdul Kadar Muhammad Masum. 2023. Human Activity Recognition Using Ensemble of CNN-Based Transfer Learning Models. In *2023 IEEE International Conference on Computing (ICOCO)*. IEEE, 112–117.
- [Kingma and Ba(2014)] Diederik P Kingma and Jimmy Ba. 2014. Adam: A method for stochastic optimization. *arXiv preprint arXiv:1412.6980* (2014).
- [Kleinsasser et al.(2022)] Maxwell Kleinsasser, Bronson Tharpe, Neelam Akula, Harshitha Tirumani, Rajshekhar Sunderraman, and Anu G Bourgeois. 2022. Detecting and Predicting Sleep Activity using Biometric Sensor Data. In *2022 14th International Conference on COMMunication Systems & NETWORKS (COMSNETS)*. IEEE, 19–24.
- [Kushwaha et al.(2021)] Amit Kumar Kushwaha, Arpan Kumar Kar, and Yogesh K Dwivedi. 2021. Applications of big data in emerging management disciplines: A literature review using text mining. *International Journal of Information Management Data Insights* 1, 2 (2021), 100017.
- [Lara and Labrador(2012)] Oscar D Lara and Miguel A Labrador. 2012. A survey on human activity recognition using wearable sensors. *IEEE communications surveys & tutorials* 15, 3 (2012), 1192–1209.

- [Lövdal et al.(2021)] SS Lövdal et al. 2021. Injury prediction in competitive runners with mach... *ijspp* 2020 (2021), 0518.
- [Luo et al.(2021)] Xiaomin Luo, Haijun Gao, Xingxia Yu, Zongping Jiang, and Weize Yang. 2021. Spectral analysis of heart rate variability for trauma outcome prediction: an analysis of 210 ICU multiple trauma patients. *European Journal of Trauma and Emergency Surgery* 47 (2021), 153–160.
- [Mao et al.(2023)] Yaxin Mao, Lamei Yan, Hongyu Guo, Yujie Hong, Xiaocheng Huang, and Youwei Yuan. 2023. A Hybrid Human Activity Recognition Method Using an MLP Neural Network and Euler Angle Extraction Based on IMU Sensors. *Applied Sciences* 13, 18 (2023), 10529.
- [Ramanujam et al.(2021)] Elangovan Ramanujam, Thinagaran Perumal, and S Padmavathi. 2021. Human activity recognition with smartphone and wearable sensors using deep learning techniques: A review. *IEEE Sensors Journal* 21, 12 (2021), 13029–13040.
- [Ramasamy Ramamurthy and Roy(2018)] Sreenivasan Ramasamy Ramamurthy and Nirmalya Roy. 2018. Recent trends in machine learning for human activity recognition—A survey. *Wiley Interdisciplinary Reviews: Data Mining and Knowledge Discovery* 8, 4 (2018), e1254.
- [Salian and Kulkarni(2023)] Preethi Salian and Sanjeev Kulkarni. 2023. Group Activity Recognition in Visual Data Using Deep Learning Framework. In *2023 2nd International Conference on Futuristic Technologies (INCOFT)*. IEEE, 1–6.
- [Weiss et al.(2019)] Gary M Weiss, Kenichi Yoneda, and Thajer Hayajneh. 2019. Smartphone and smartwatch-based biometrics using activities of daily living. *Ieee Access* 7 (2019), 133190–133202.
- [Woznowski et al.(2016)] Przemyslaw Woznowski, Rachel King, William Harwin, and Ian Craddock. 2016. A human activity recognition framework for healthcare applications: ontology, labelling strategies, and best practice. In *International Conference on Internet of Things and Big Data*, Vol. 2. SciTePress, 369–377.
- [Xie et al.(2024)] Zhao Xie, Chang Jiao, Kewei Wu, Dan Guo, and Richang Hong. 2024. Active Factor Graph Network for Group Activity Recognition. *IEEE Transactions on Image Processing* (2024).
- [Yu et al.(2019)] Yong Yu, Xiaosheng Si, Changhua Hu, and Jianxun Zhang. 2019. A review of recurrent neural networks: LSTM cells and network architectures. *Neural computation* 31, 7 (2019), 1235–1270.
- [Zhang et al.(2022)] Shibo Zhang, Yaxuan Li, Shen Zhang, Farzad Shahabi, Stephen Xia, Yu Deng, and Nabil Alshurafa. 2022. Deep learning in human activity recognition with wearable sensors: A review on advances. *Sensors* 22, 4 (2022), 1476.

A Appendices

ID	Amount of missing data	Amount of missing data imputed as sleeping	Amount of missing data imputed as awake	Amount of data not able to be imputed	Percentage of missing data imputed as sleeping	Percentage of missing data imputed as awake	Percentage of missing data not able to be imputed	Percentage of overall data that was imputed
1	5823	2204	2909	710	37.85	49.96	12.19	71.01
2	141583	62409	78678	496	44.08	55.57	0.35	77.76
3	6126	1017	3888	1221	16.6	63.47	19.93	68.12
4	81538	30487	50167	884	37.39	61.53	1.08	82.37
5	85543	50764	33400	1379	59.34	39.04	1.61	81.18
6	12837	3279	8940	618	25.54	69.64	4.81	77.14
7	12626	2723	9362	541	21.57	74.15	4.28	76.29
8	82959	35543	46964	452	42.84	56.61	0.54	79.58
9	99043	53795	44692	556	54.31	45.12	0.56	79.53
10	84891	28316	55253	1322	33.36	65.09	1.56	79.5
11	76223	35315	39367	1541	46.33	51.65	2.02	78.58
12	78718	38151	39841	726	48.47	50.61	0.92	82.06
13	15944	5626	9981	337	35.29	62.6	2.11	83.37
14	126344	36085	89058	1201	28.56	70.49	0.95	77.59
15	49848	21466	27032	1350	43.06	54.23	2.71	78.32
16	7272	2682	3515	1075	36.88	48.34	14.78	71.72
17	34231	21671	11612	948	63.31	33.92	2.77	79.7
18	9370	4084	5284	2	43.59	56.39	0.02	81.32
19	91568	40342	50644	582	44.06	55.31	0.64	77.05
20	17863	7453	9097	1313	41.72	50.93	7.35	76.62
21	36769	14431	21628	710	39.25	58.82	1.93	80.78
22	126500	48050	77602	848	37.98	61.35	0.67	79.33
23	114394	56025	57728	641	48.98	50.46	0.56	77.45
24	107279	31503	75343	433	29.37	70.23	0.4	81.54
25	136083	43320	91911	852	31.83	67.54	0.63	77.61
26	101055	26016	73837	1202	25.74	73.07	1.19	78.8
27	1320	80	681	559	6.06	51.59	42.35	52.85
28	130692	52712	76116	1864	40.33	58.24	1.43	79.88
29	2560	184	1562	814	7.19	61.02	31.8	60.62
30	28409	13711	13664	1034	48.26	48.1	3.64	79.21
31	27384	12193	14498	693	44.53	52.94	2.53	77.23
32	22539	9233	12785	521	40.96	56.72	2.31	80.48
33	63237	24126	38547	564	38.15	60.96	0.89	77.72
34	68189	25416	40937	1836	37.27	60.03	2.69	75.54
35	47005	20108	25690	1207	42.78	54.65	2.57	77.57
36	141307	85982	54789	536	60.85	38.77	0.38	81.46
37	12059	5224	5635	1200	43.32	46.73	9.95	75.41
38	31213	11841	18112	1260	37.94	58.03	4.04	80
39	64472	22237	41563	672	34.49	64.47	1.04	77.73
40	79211	34163	43536	1512	43.13	54.96	1.91	77.08
41	109153	45658	62864	631	41.83	57.59	0.58	76.12
42	9720	1552	6827	1341	15.97	70.24	13.8	72.73
43	128817	64353	63575	889	49.96	49.35	0.69	78.62
44	87779	33146	52623	2010	37.76	59.95	2.29	76.36
45	112731	50600	61684	447	44.89	54.72	0.4	78.76
46	93269	42183	50381	705	45.23	54.02	0.76	80.35
47	2617	586	1546	485	22.39	59.08	18.53	74.03
48	9777	2428	6643	706	24.83	67.95	7.22	78.74
49	97694	33568	63544	582	34.36	65.04	0.6	77.52
50	10519	5710	4179	630	54.28	39.73	5.99	76.3
51	58882	19490	38841	551	33.1	65.96	0.94	81.02
52	27631	10578	15685	1368	38.28	56.77	4.95	79.3
53	57032	26008	30319	705	45.6	53.16	1.24	79.83
54	2658	297	1573	788	11.17	59.18	29.65	64.93
55	101202	26789	73985	428	26.47	73.11	0.42	76.9
56	69351	31494	37331	526	45.41	53.83	0.76	78.35
57	180491	77262	101840	1389	42.81	56.42	0.77	79.73
58	51793	9715	40866	1212	18.76	78.9	2.34	78.06
59	9470	2316	6457	697	24.46	68.18	7.36	76.15
60	15965	10473	4899	593	65.6	30.69	3.71	82.12
61	2621	231	1370	1020	8.81	52.27	38.92	55.59
62	77982	30028	47784	170	38.51	61.28	0.22	83.13
63	225463	103702	121400	361	46	53.84	0.16	80.16
64	4755	644	3498	613	13.54	73.56	12.89	71.91
65	129450	49094	79651	705	37.93	61.53	0.54	77.07
66	10129	1359	8242	528	13.42	81.37	5.21	74.08
67	16389	11926	3263	1200	72.77	19.91	7.32	75.34
68	68815	41316	26292	1207	60.04	38.21	1.75	76.97
69	151867	69478	81012	1377	45.75	53.34	0.91	77.99
70	65120	33966	30042	1112	52.16	46.13	1.71	77.98
71	29824	17753	10314	1757	59.53	34.58	5.89	74.97
72	80271	39794	40000	477	49.57	49.83	0.59	75.91
73	69165	31481	36273	1411	45.52	52.44	2.04	81.12
74	136601	64995	70346	1260	47.58	51.5	0.92	80.33
75	17619	7232	9423	964	41.05	53.48	5.47	77.11
76	8444	2726	4254	1464	32.28	50.38	17.34	69.25
77	71263	47296	22685	1282	66.37	31.83	1.8	79.67
78	16369	9993	5341	1035	61.05	32.63	6.32	81.91
79	41388	34568	32	6788	83.52	0.08	16.4	70.67

Table 2: Imputation stats for each soldier part I

ID	Amount of missing data	Amount of missing data imputed as sleeping	Amount of missing data imputed as awake	Amount of data not able to be imputed	Percentage of missing data imputed as sleeping	Percentage of missing data imputed as awake	Percentage of missing data not able to be imputed	Percentage of overall data that was imputed
80	14548	4905	8459	1184	33.72	58.15	8.14	77.34
81	124296	47683	75697	916	38.36	60.9	0.74	75.82
82	115122	43642	70597	883	37.91	61.32	0.77	81.79
83	7274	2024	4199	1051	27.83	57.73	14.45	72.03
84	35375	13839	19538	1998	39.12	55.23	5.65	77.26
85	66619	30501	35534	584	45.78	53.34	0.88	80.45
86	102955	50043	51712	1200	48.61	50.23	1.17	77.65
87	10775	3238	5896	1641	30.05	54.72	15.23	70.48
88	57768	18202	38246	1320	31.51	66.21	2.29	80
89	165685	32662	132610	413	19.71	80.04	0.25	81.98
90	35479	18954	16289	236	53.42	45.91	0.67	78.95
91	126869	40752	85635	482	32.12	67.5	0.38	78.36
92	59280	39757	18188	1335	67.07	30.68	2.25	77.38
93	108415	88327	19870	218	81.47	18.33	0.2	81.67
94	6345	2047	3468	830	32.26	54.66	13.08	76.6
95	12919	5628	6868	423	43.56	53.16	3.27	78.89
96	153531	60382	91916	1233	39.33	59.87	0.8	78.93
97	137665	46749	90515	401	33.96	65.75	0.29	80.78
98	125985	44037	81258	690	34.95	64.5	0.55	79.1
99	78665	30935	46530	1200	39.32	59.15	1.53	79.11
100	2523	340	1352	831	13.48	53.59	32.94	58.75
101	3696	249	2745	702	6.74	74.27	18.99	69.31
102	131105	42708	87953	444	32.58	67.09	0.34	77.55
103	59322	35451	20348	3523	59.76	34.3	5.94	79.08
104	31243	11342	19310	591	36.3	61.81	1.89	78.84
105	6373	4177	936	1260	65.54	14.69	19.77	71.01
106	92763	39012	53316	435	42.06	57.48	0.47	78.19
107	153186	76196	76401	589	49.74	49.87	0.38	80.89
108	9173	2321	6788	64	25.3	74	0.7	79.07
109	58442	32686	24907	849	55.93	42.62	1.45	81.62
110	116232	46232	69378	622	39.78	59.69	0.54	77.95
111	84771	30263	54508	0	35.7	64.3	0	80.64
112	7286	2699	4201	386	37.04	57.66	5.3	79.86
113	48699	32140	15486	1073	66	31.8	2.2	80.67
114	74961	22574	51650	737	30.11	68.9	0.98	80.54
115	13133	3846	4591	4696	29.29	34.96	35.76	53.26
116	111355	40220	69797	1338	36.12	62.68	1.2	77.96
117	8274	1632	4948	1694	19.72	59.8	20.47	65.28
118	94219	41474	51400	1345	44.02	54.55	1.43	82.69
119	50885	38069	11030	1786	74.81	21.68	3.51	75.77
120	10368	1698	7853	817	16.38	75.74	7.88	73.7
121	14804	7322	1895	5587	49.46	12.8	37.74	53.34
122	29812	15400	13125	1287	51.66	44.03	4.32	79.24
Average	62953.34	26755.02	35161.27	1037.05	39.91	54.35	5.74	76.67

Table 3: Imputation stats for each soldier part II